

PL-TR--93-2109
Instrumentation Papers, No. 346

ADVANCED RETROREFLECTIVE TELESCOPE BAFFLE

E. Ray Huppi
Roy A. Austin

14 May 1993

19980202 038

APPROVED FOR PUBLIC RELEASE; DISTRIBUTION UNLIMITED.

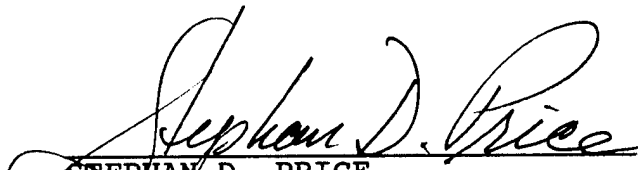


PHILLIPS LABORATORY
Directorate of Geophysics
AIR FORCE MATERIEL COMMAND
HANSCOM AIR FORCE BASE, MA 01731-3010

DHC QUALITY INSPECTED 3

This technical report has been reviewed and is approved for publication


ERNEST R. HUPPI
Author


STEPHAN D. PRICE
Branch Chief


ROGER VAN TASSEL
Division Director

This report has been reviewed by the ESC Public Affairs Office (PA) and is releasable to the National Technical Information Service (NTIS).

Qualified requestors may obtain additional copies from the Defense Technical Information Center. All others should apply to the National Technical Information Service.

If your address has changed, or if you wish to be removed from the mailing list, or if the addressee is no longer employed by your organization, please notify PL/TSI, Hanscom AFB, MA 01731-3010. This will assist us in maintaining a current mailing list.

Do not return copies of this report unless contractual obligations or notices on a specific document requires that it be returned.

REPORT DOCUMENTATION PAGE			Form Approved OMB No. 0704-0188	
Public reporting burden for this collection of information is estimated to average 1 hour per response, including the time for reviewing instructions, searching existing data sources, gathering and maintaining the data needed, and completing and reviewing the collection of information. Send comments regarding this burden estimate or any other aspect of this collection of information, including suggestions for reducing this burden, to Washington Headquarters Services, Directorate for Information Operations and Reports, 1215 Jefferson Davis Highway, Suite 1204, Arlington, VA 22202-4302, and to the Office of Management and Budget, Paperwork Reduction Project (0704-0188), Washington, DC 20503.				
1. AGENCY USE ONLY (Leave blank)	2. REPORT DATE 14 May 1993	3. REPORT TYPE AND DATES COVERED Scientific, Final (July 1991-July 1992)		
4. TITLE AND SUBTITLE Advanced Retroreflective Telescope Baffle		5. FUNDING NUMBERS PE 61101F PR ILIR TA 1A WU 01		
6. AUTHOR(S) E. Ray Huppi Roy A. Austin				
7. PERFORMING ORGANIZATION NAME(S) AND ADDRESS(ES) Phillips Laboratory (GPOB) 29 Randolph Rd Hanscom AFB, MA 01731-3010		8. PERFORMING ORGANIZATION REPORT NUMBER PL-TR-93-2109 I.P., No. 346		
9. SPONSORING/MONITORING AGENCY NAME(S) AND ADDRESS(ES)		10. SPONSORING/MONITORING AGENCY REPORT NUMBER		
11. SUPPLEMENTARY NOTES Phillips Laboratory POC: E. Ray Huppi/GPOB x-3715				
12a. DISTRIBUTION AVAILABILITY STATEMENT Approved for public release; Distribution unlimited		12b. DISTRIBUTION CODE		
13. ABSTRACT (Maximum 200 words) Optical baffle designs that incorporate arrays of small cell cube corner retroreflectors to reflect off-axis rays back out the entrance aperture of the baffle are discussed. Laboratory measurements of the optical properties of a cube corner array were made and the results presented. The reflection, absorption and transmission of baffles utilizing cube corner arrays were calculated using PC GUERAP and the results compared to a standard black absorbing baffle design. The reflective baffle designs evaluated are able to reflect from 40 to 80 percent of off-axis rays, thus significantly decreasing the energy absorbed by the baffle. Baffles utilizing arrays of cube corner reflectors could potentially be used in space based infrared surveillance sensors to reduce cooling requirements.				
14. SUBJECT TERMS Reflective baffle, Cube corner arrays			15. NUMBER OF PAGES 40	
			16. PRICE CODE	
17. SECURITY CLASSIFICATION OF REPORT Unclassified	18. SECURITY CLASSIFICATION OF THIS PAGE Unclassified	19. SECURITY CLASSIFICATION OF ABSTRACT Unclassified	20. LIMITATION OF ABSTRACT SAR	

Contents

1	INTRODUCTION	1
2	APPROACH	3
3	DISCUSSION	3
4	SUMMARY AND CONCLUSIONS	28
	REFERENCES	33

Illustrations

1	Two different types of cube corner arrays.	5
2	Cube corner coordinate system.	8
3	Retroreflection efficiency as a function of incident angle.	9
4	The exit angle of two-reflection rays as a function of incident angle.	11
5	Relative energy contained in single reflection and double reflection beams.	12
6	Relative energy contained in single reflection and double reflection beams.	14
7	Measured diffuse scatter of cube corner array.	15
8	Retroreflecting baffle.	17
9	Baseline black baffle.	19
10	Fraction of energy reflected back out the entrance .	20
11	Fraction of energy absorbed.	21
12	Fraction of energy transmitted.	22
13	Fraction of energy reflected back out entrance.	25
14	Fraction of energy absorbed.	26
15	Fraction of energy transmitted	27
16	Modified baffle design having a reflecting entrance aperture.	30
17	Fraction of energy reflected.	31
18	Fraction of energy transmitted.	32

Acknowledgements

We would like to thank Dr. George Vanasse and Donald Smith for their suggestions and many illuminating discussions. We would also like to thank Capt. Deborah Dean for her help with the laboratory measurements.

Advanced Retroreflective Telescope Baffle

1. INTRODUCTION

For a number of years, the Geophysics Directorate of Phillips Laboratory has been involved in an on-going program to measure high altitude atmospheric infrared backgrounds. The measurements are being made with rocket and satellite borne infrared optical sensors cooled with liquid helium. The purpose of these measurements is to determine the spatial and spectral characteristics of infrared backgrounds that will be viewed by future space based above the horizon infrared surveillance systems designed to detect and track ICBM targets during midcourse flight. The infrared radiation from the upper atmosphere is orders of magnitude lower than the radiation from the earth and lower atmosphere, and therefore, the sensors must be cooled to low temperature to eliminate self emission and must have a baffle and telescope that has very high off-axis rejection. The standard approach is to use an all reflective telescope with super polished low scatter mirrors behind a baffle painted with absorbing diffuse black paint. The purpose of the baffle is to absorb off-axis radiation and thus prevent it from hitting and scattering from the telescope mirrors. This approach

has worked well, but there has always been off-axis leakage of earth and lower atmospheric radiation that is detected above the noise level of the sensor. The off-axis leakage makes it difficult to measure the true emission spectrum of the upper atmosphere since spectral emission and absorption features of the lower atmosphere contaminate the true spectrum. This is especially true at very high altitudes where the emission from the atmosphere is very weak. In addition, the black paint used for the baffle coating is not always equally absorbing at all wavelengths, which can result in spectral features of the baffle paint in the off-axis leakage spectrum.

The telescope diameter must be relatively large (10 to 20 inches) to obtain good spatial resolution and the high sensitivity required to measure emissions from the rarefied upper atmosphere. The large diameter requires the baffle to absorb a significant amount of thermal radiation coming from the earth and lower atmosphere as well as from direct and scattered solar illumination. This heat load is not a significant problem for a sounding rocket sensor since the measurement time is short, but it has significant impact on the cryogen consumption or the power required for sensor refrigeration for a satellite borne sensor required to operate in space for an extended time period.

The purpose of this Laboratory Directors Fund sponsored effort was to address both the baffle off-axis leakage and the baffle heat load problems, and specifically to investigate the use of small cell, cube corner retroreflector arrays as a coating for forward facing baffle surfaces instead of the standard diffuse black paint. A good black paint will typically absorb about 95 percent of the incident energy and diffusely reflect 5 percent. A cube corner retroreflector array can reflect a significant fraction of incident radiation directly back to the source, thus reducing the energy absorbed by the baffle. If a significant portion of the radiation that enters the baffle is reflected back out the entrance aperture, then there is also the potential for reducing the amount of off-axis radiation

transmitted through the baffle. This could result in a reduction of off axis leakage since there would be less radiation available to scatter from the telescope optical elements.

2. APPROACH

Our investigation involved three steps. First, a literature search was conducted to find out what was known about the properties of cube corner reflectors and cube corner arrays. Second, samples of cube corner arrays were obtained from several sources, and laboratory optical measurements were made on the array samples. Third, the array type that showed the most promise was selected for more extensive testing and a computer model of the cube corner array was developed and incorporated into a commercially available stray light ray trace program (PC GUERAP). The performance of a baffle utilizing baffle rings covered with cube corner arrays was then calculated using the ray trace program. The absorption, transmission and retroreflection of the baffle were calculated as a function of off-axis angle. The baffle design was then modified in an attempt to minimize both the off-axis transmission and absorption. The calculated results for the cube corner baffle were compared to calculations of a similar baffle painted with diffuse black paint.

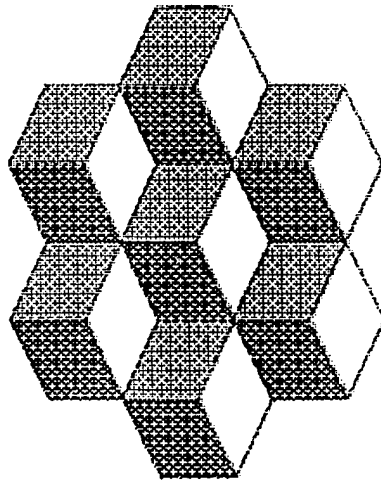
3. DISCUSSION

A cube corner reflector consists of three reflecting surfaces at right angles to each other forming a corner. This arrangement of three mirrors has the property that any ray reflected from all three surfaces is exactly reversed in direction (Sears, 1949). Other names for the cube corner are retrodirective reflector,

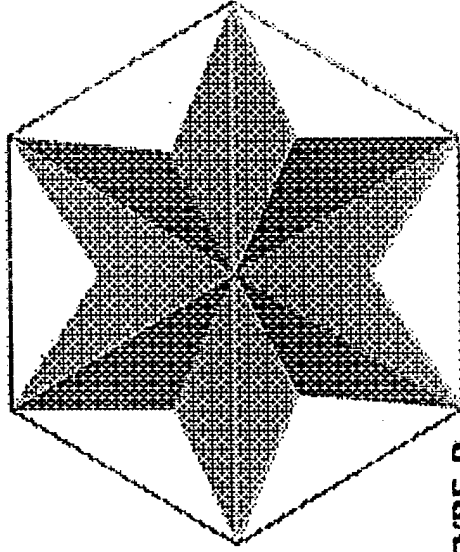
retroreflector and corner reflector. The cube corner or arrays of cube corners are often used for roadside reflectors since they efficiently reflect automobile headlamp light back to the automobile. They are also used as retrodirective targets in optical ranging systems. The cube corner can either be hollow, being formed by three front surface mirrors, or it can be made of solid optical material where the light enters the front face, makes three internal reflections, and exits the front face. In either case the light ray must reflect from all three surfaces to be retroreflected. The solid type is often used in the visible since there are suitable inexpensive optical materials that have high transmission in the visible. Cube corners for the infrared are most often of the hollow type made of three front surface mirrors.

The individual mirrors that form the corner can either be isosceles right triangles or squares. Arrays of cube corners can be made from either type as shown in Figure 1. Chipman, et. al. (1988) have pointed out that when the cube corner cell is made from three triangular mirrors, a maximum of two thirds of the incident rays will be retroreflected. Rays that enter near the three points of the cube corner cell only reflect from two surfaces before leaving the cell, and are not reflected back along the incident ray. A cube corner array made from three square mirrors can theoretically retroreflect 100 percent of incident rays for rays that are normal to the array. If incident rays are not normal to the array, then some rays exit the array with less than three reflections, and these rays are not retroreflected. As the angle of incidence is increased, the fraction of rays retroreflected decreases (Wolf and Zissis, 1985). A ray that is retroreflected is reflected back parallel to the incident ray but with some lateral displacement, the maximum displacement being the dimension of the cube corner cell. If an array of very small cube corner cells is used then the displacement is very small and the reflected ray is almost coincident with the incident ray. An array of small cell cube corners approximates a phase-conjugate mirror (Barrett and Jacobs, 1979; Jacobs, 1982).

CUBE CORNER RETRO-REFLECTION ARRAYS



**TYPE A
MORE EFFICIENT
100 % RETRO-REFLECTION
AT NORMAL INCIDENCE**



**TYPE B
LESS EFFICIENT
67 % RETRO-REFLECTION
AT NORMAL INCIDENCE**

Figure 1. Two different types of cube corner arrays. Type A made from square mirrors is more efficient than type B made from triangular mirrors.

The first retroreflector sample evaluated was a hollow cell array obtained from Reflexite Corporation. The array was originally used as a mold to produce flexible plastic retroreflecting material by hot pressing the mold into one surface of a thin sheet of plastic material. The plastic array that results is a solid cell array that is normally illuminated from the flat front surface and is not suitable for the infrared, but the mold is hollow cell and can be coated with an infrared reflecting coating such as aluminum or gold. Each cell is 150 micrometers across and consists of three triangular mirrors. The small cell size is ideal for visible light but in the infrared, diffraction would broaden the reflected beam. Also, since the cells are made from triangular mirrors the maximum retroreflection efficiency is 67 percent.

A number of hollow cell arrays with each cell made from square surfaces were obtained from The Reflectory Corp. and from 3M Corporation. The arrays were examined under the microscope for surface quality and uniformity and one array was selected for more extensive testing. The selected array was 2 inches in diameter with a 0.1 inch cell spacing. The array was obtained from 3M Corporation and was originally designed for use as a roadside reflector. The array normally would be used as a solid cell array illuminated from the flat front side. For use in the infrared, the protective back cover of the array was removed to expose the hollow cell back side of the array. The hollow cell array was then coated with an evaporated aluminum reflective film so that each surface of each cell became a front surface mirror.

The retroreflecting and "stray" two-reflection and single-reflection properties of the array were evaluated by illuminating the array with a collimated beam of light over a range of incidence angles. The angle of incidence was varied by tilting the array. The power in the retroreflected beams and the stray beams was measured as a function of incidence angle. The sample holder could be tilted in either direction as well as rotated. It was determined that the direction and

power of the stray two-reflection and single-reflection beams depended on the orientation of the cube corner cell mirrors relative to the incident beam. A coordinate system was defined to better understand and interpret the measured results. Each cube corner cell contains three lines of intersection formed where any two surfaces intersect. Figure 2 shows one cell of a cube corner array, the cell being formed from three square mirrors. The three lines of intersection meet at point O and are shown in the figure as OA, OB, and OC. Each line of intersection is perpendicular to one of the three mirror surfaces. The normal to the array is defined as all lines that are parallel to a line passing through O and having equal angular distance from the three lines of intersection. A positive incidence angle is defined as the angle between the incident ray and the normal to the array when the incident ray is tilted toward the line of intersection OA. At a positive angle of 54.74 degrees the incident ray is parallel to the line OA and is therefore parallel to the two mirrors that form the intersection (surfaces 1 and 2) and normal to the other mirror (surface 3). For incident rays with a positive angle of 54.74 degrees or larger all rays only reflect from surface 3. A negative incidence angle is defined as an angle away from the line of intersection OA. At a negative angle of 35.26 degrees all incident rays are parallel to mirror surface 3, and all rays are reflected two times, once from surface 1 and once from surface 2. At negative angles with magnitude greater than 35.26 degrees three-surface reflection is no longer possible.

The laboratory measurement of normalized retroreflection efficiency as a function of incidence angle is shown in Figure 3. The sample tested had only a maximum retroreflection efficiency of 0.33, with transmission through the reflective coating, scatter, and absorption accounting for 67 percent. The figure shows a nearly linear decrease in retroreflection efficiency as the magnitude of the incident angle is increased. The efficiency goes to zero at about 55 degrees for positive incidence angles and at about 35 degrees for negative incidence angles.

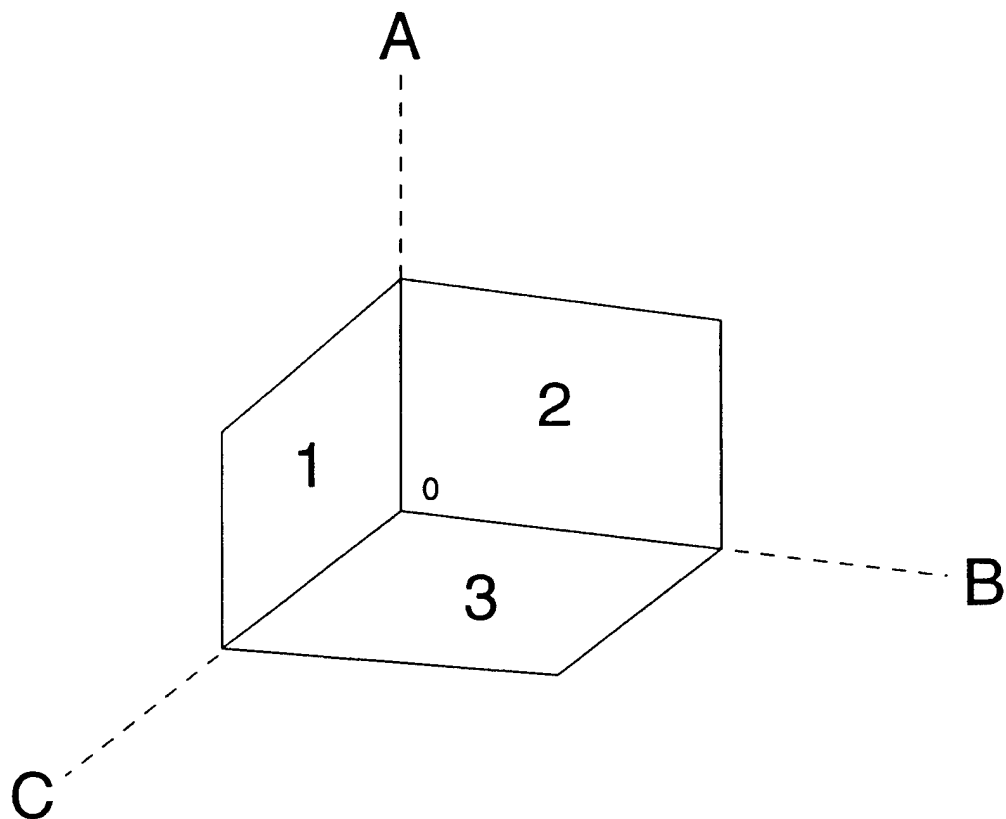


Figure 2. Cube corner coordinate system

MEASURED RETRO-REFLECTION EFFICIENCY

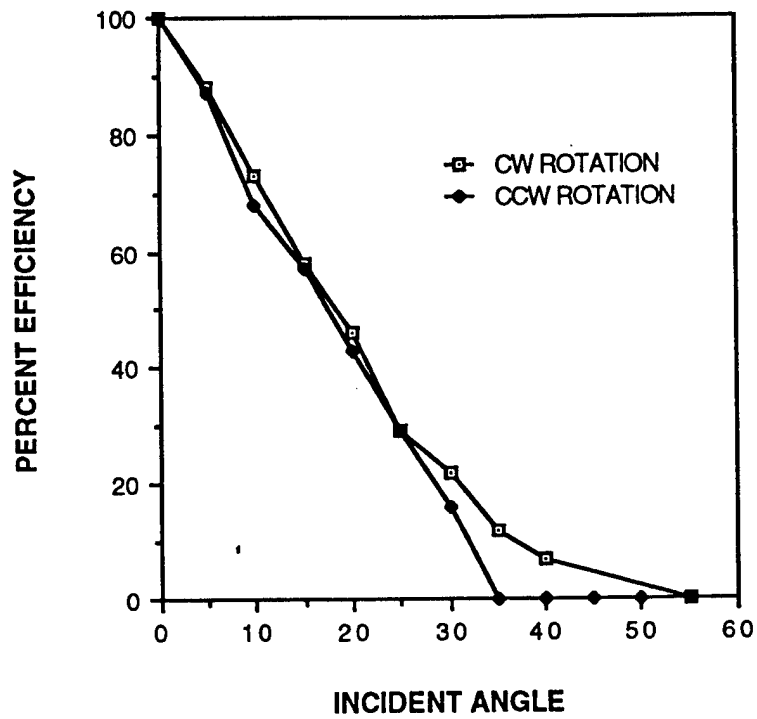


Figure 3. Retroreflection efficiency as a function of incident angle.

For small incidence angles very near normal incidence, most rays are reflected from all three mirror surfaces and are retroreflected. Some rays, however, only reflect from two surfaces and exit the array at angles considerably away from the retroreflected rays. For very small incidence angles the two-reflection rays exit at about 70 degrees from the normal. The angle of reflection for two-reflection rays (beams A, B and C) and for single-reflection rays (beam D) is shown in Figure 4 for a range incidence angles. The fact that the two reflection rays can exit at such large angles is an undesirable characteristic in a baffle application since rays that exit at large angles are not easily directed back out the baffle entrance and must be absorbed by the baffle. When designing a baffle that incorporates cube corner retroreflectors, attention must be given to what happens to two-reflection and single-reflection rays. Fortunately, as will be shown in the discussion that follows, the number of rays that exit the array at a large angle is small.

The relative energy contained in two-reflection and single-reflection rays as a function of incidence angle is shown in Figure 5. The energy in the two-reflection rays is minimum at zero incidence angle. This is as expected since almost all rays at near zero incidence angle will experience three reflections and be retroreflected. At negative incidence angles there is no energy in two-reflection beams B and C or single-reflection beam D, and the energy in beam A increases almost linearly with angle until a maximum is reached at 35.26 degrees. At this point all incident rays experience two reflections. From figure 4 it is seen that the angle of incidence and the angle of reflection are the same at 35.26 degrees. At this angle the array acts as an array of roof mirrors and all rays are again retroreflected back toward the source. For positive incidence angles there is no energy in beam A. The energy increases in beam B and C with increasing angle and peaks at about 30 degrees and then decreases with further increase in angle. As the energy in B and C decrease the energy is given up to

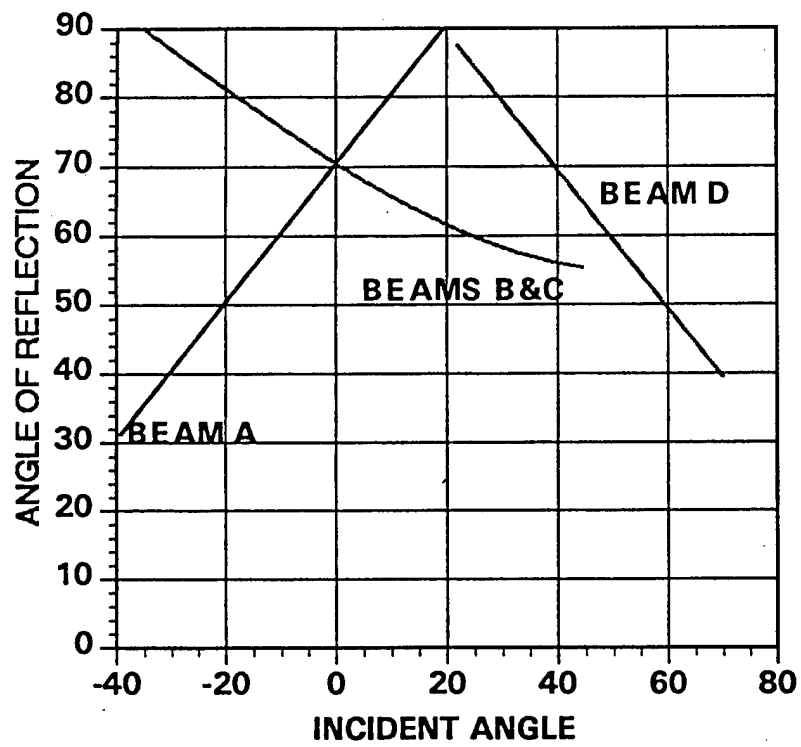


Figure 4. The exit angle of two-reflection rays as a function of incident angle.

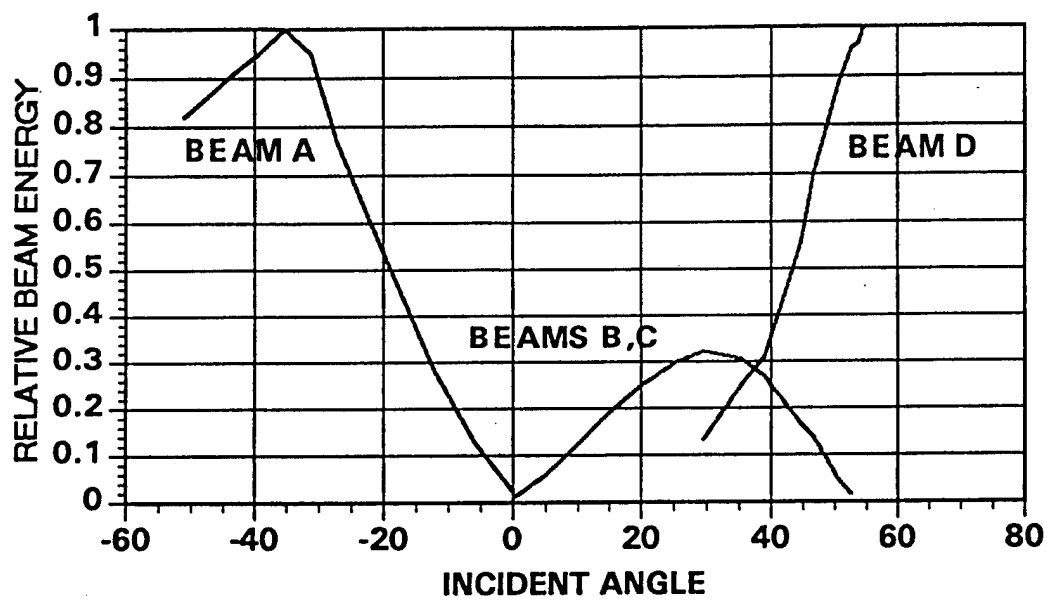


Figure 5. Relative energy contained in single reflection and double reflection beams.

single reflection beam D. At a positive angle of 54.74 degrees, all rays experience only a single reflection. At this point the array acts as an array of flat mirrors that are perpendicular to the incident rays and once again all rays are reflected back to the source. It is important to note that as the energy in beams A and D increase the angle between the incident and reflected rays decreases, which results in most of the one-reflection and two-reflection rays being directed back toward the incident rays. This is shown in Figure 6 which is a plot of the relative energy in the beams as a function of the angle (γ) between the incident and reflected rays.

The relative energy measured in the two-reflection rays is lower than expected due to relatively high absorption and scatter of the reflective surfaces. The reflective coating on the array is an evaporated aluminum coating that was expected to have 95 percent or greater reflection in the visible and infrared. Our measurements indicate that 16 percent was either absorbed or transmitted through the coating per reflection.

The radiation scattered from the array was measured as a function of scatter angle with the array illuminated by a collimated beam normal to the array. The measured results are shown in Figure 7. The scattered radiation contains a diffuse component and a non-diffuse component. The diffuse component results from imperfections in the surfaces of cube corner cells and imperfections in the reflective coating. The non-diffuse component is the result of the finite radius that exists at the intersection of the three surfaces that form a cube corner cell and from the finite radius that exists where one cell joins another cell. The total diffuse scatter was determined to be 12 percent. This is higher than desired but consistent with the fact that the array, being a roadside reflector, was not designed to minimize scattered radiation. The non-diffuse component could not be measured accurately but a calculation based on a measured edge radius of 0.004 inches resulted in 16 percent scatter from surface intersections. It was

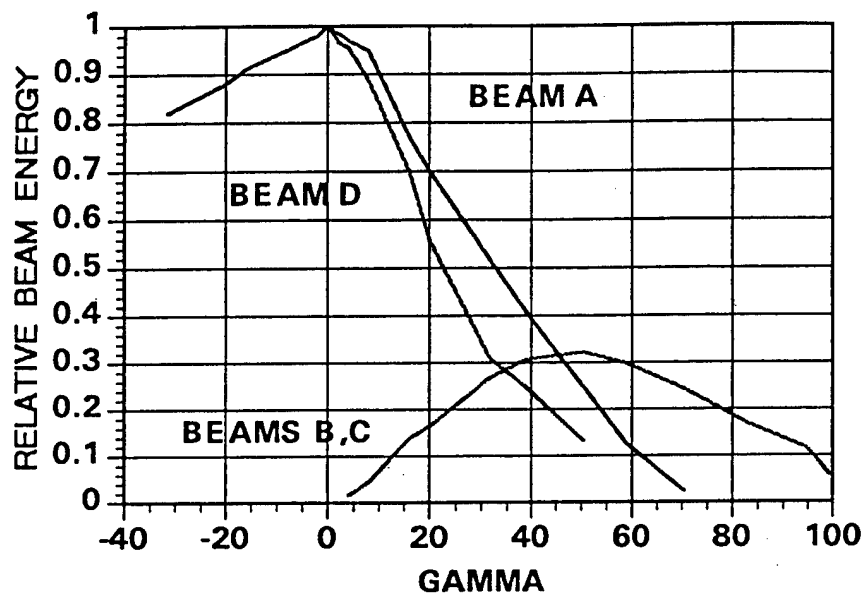


Figure 6. Relative energy contained in single reflection and double reflection beams plotted as a function of the angle between the incident and reflected beams.

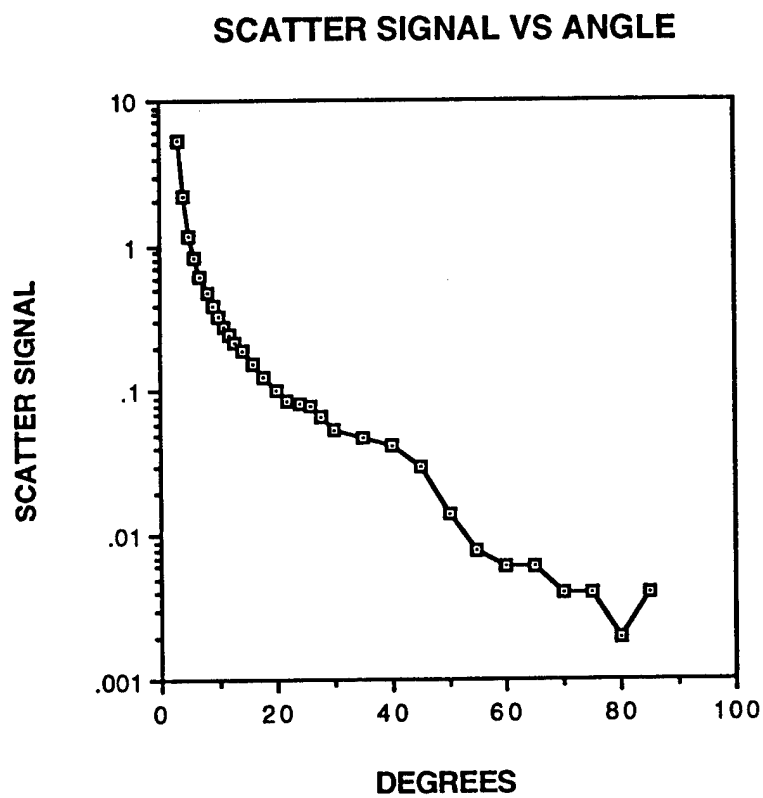


Figure 7. Measured diffuse scatter of a cube corner array as a function of scatter angle.

beyond the scope and budget of this effort to have arrays with lower scatter made, but scatter would be expected to be lower with greater care in the manufacture of the cube corner arrays.

After gaining an understanding of retroreflection efficiency and the direction and intensity of non-retroreflected rays, the next step was to develop a computer model of the array and incorporate the model into a stray light ray trace program. The program we selected is PC GUERAP which is commercially available from Teloptic Corp. of Sudbury Massachusetts. Teloptic Corp. also developed the model for the cube corner array. The program allows the user to specify the absorption that occurs at each surface reflection as well as a diffuse reflection component. The non-diffuse scatter from the cube corner intersections was not incorporated into the model.

A baffle utilizing cube corner arrays was designed and is shown in Figure 8. The baffle has an exit aperture diameter of 1 inch and an overall length of 10 inches. The front surfaces of the baffle rings facing toward the entrance aperture are covered with cube corner arrays. The baffle rings are angled so that the baffle surface is approximately normal to rays that strike the baffle ring after passing through the entrance aperture. The ring spacing is arranged so that all rays that do not pass to the exit aperture directly must strike a retroreflecting surface. The baffle barrel and the back side of all rings are covered with diffuse black paint that absorbs 95 percent of incident rays and scatters 5 percent. The edges of all rings are sharpened knife edges having a edge radius of 0.001 inch. Any ray that is either scattered from the cube corner surfaces or that exits the array cells with less than three reflections (two-reflection and single-reflection rays) must make at least two reflections from a black surface before reaching the exit aperture.

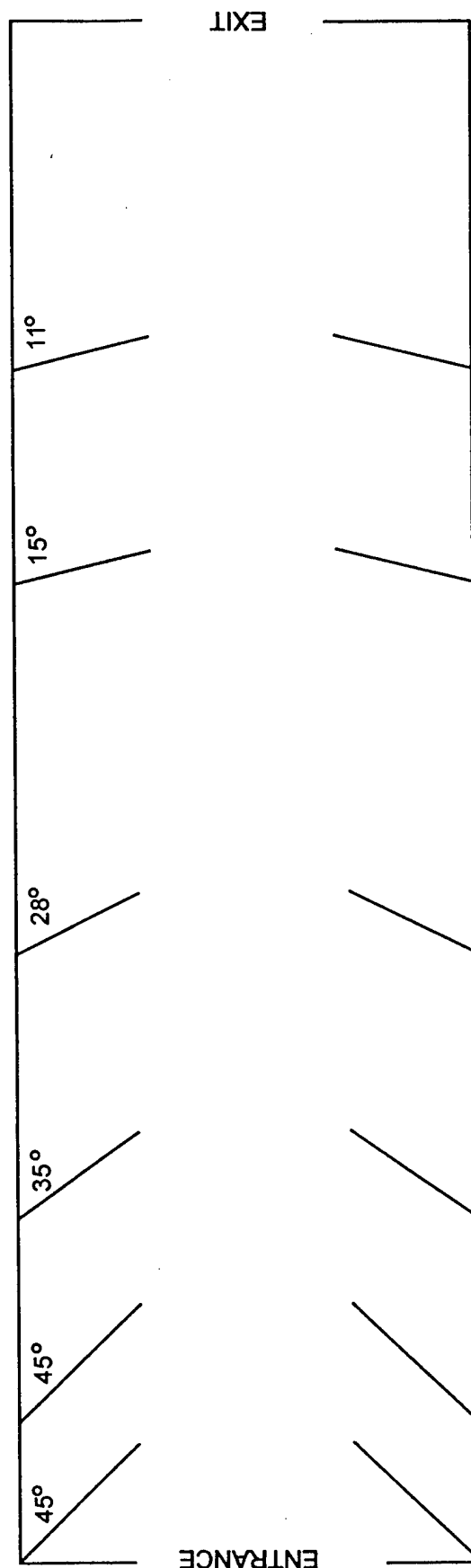


Figure 8. Retroreflecting baffle. Entrance aperture is at left and exit aperture is at right. Baffle ring surfaces facing entrance are covered with retroreflecting cube corner arrays. Baffle ring back surfaces and baffle tube are painted with black diffuse paint.

A standard black absorbing baffle having the same basic dimensions was also designed so that the performance of the reflective baffle could be compared to the performance of a standard black baffle. The black absorbing baffle is shown in Figure 9. The baffle rings are placed so that any ray that does not pass directly through to the exit aperture must have a minimum of two reflections before reaching the exit aperture. Exceptions to this requirement are rays that reflect from the knife edges of the baffle rings. The baffle ring edges are sharpened to a radius of 0.001 inch and are highly reflective so it is possible for some rays to make a single reflection from a baffle edge and exit the baffle. The fraction of incident rays reflected back out the entrance, the fraction transmitted to the exit aperture and the fraction absorbed by the baffle were computed for a range of incidence angles for a number of retroreflecting baffle designs, and the results were compared to similar calculations for the baseline black baffle. The basic retroreflecting baffle design remained similar in geometry with only slight variations. Variations were made in the number of baffle rings that were covered with retroreflecting cells as well as slight changes in the angle of some baffle rings. Baffle designs with and without the entrance aperture were considered. Without the entrance aperture the fraction of rays which are absorbed and transmitted by the baffle decreases, but since the total area exposed to off-axis radiation is increased, the total energy that must be absorbed by the baffle increases. The baffle shown in Figure 8 resulted in the best overall performance of the variations tried for baffles which have a flat entrance aperture.

The calculated results for a reflecting design and the baseline black design are shown in Figures 10, 11, and 12. The reflecting baffle had cube corner arrays on all baffle ring surfaces facing toward the entrance aperture. No absorption or scatter was assumed for the cube corner arrays used in the reflective baffle. This was done to find out how well the retroreflecting baffle would perform with ideal cube corners. The baffle tube, the back side of all baffle rings, and the back side

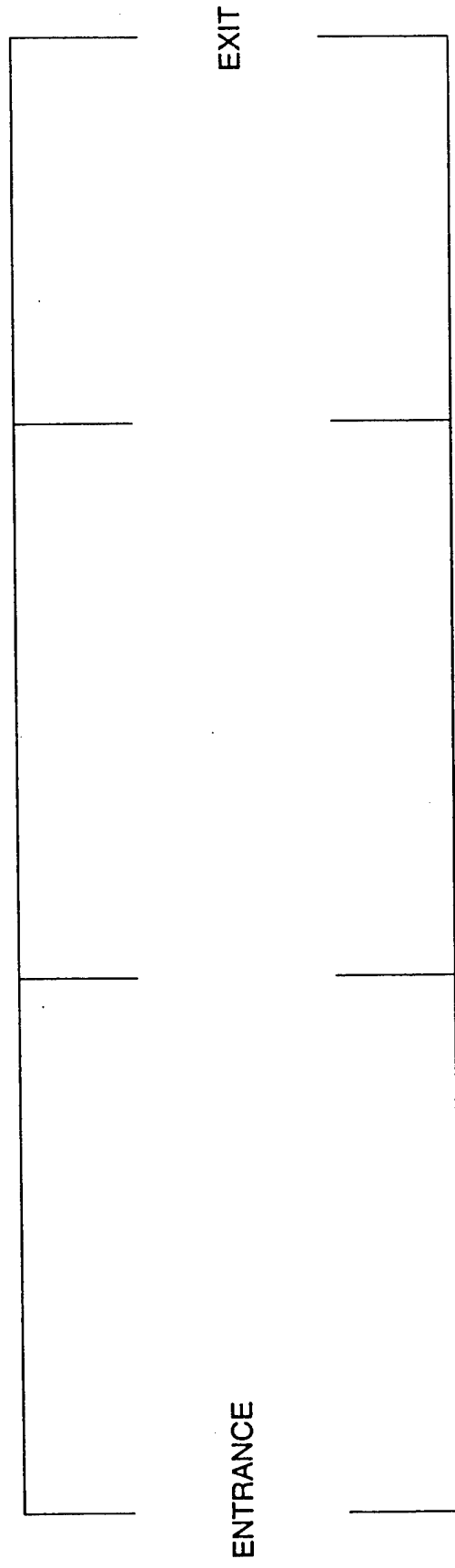


Figure 9. Baseline black baffle. All surfaces are painted with black diffuse paint.

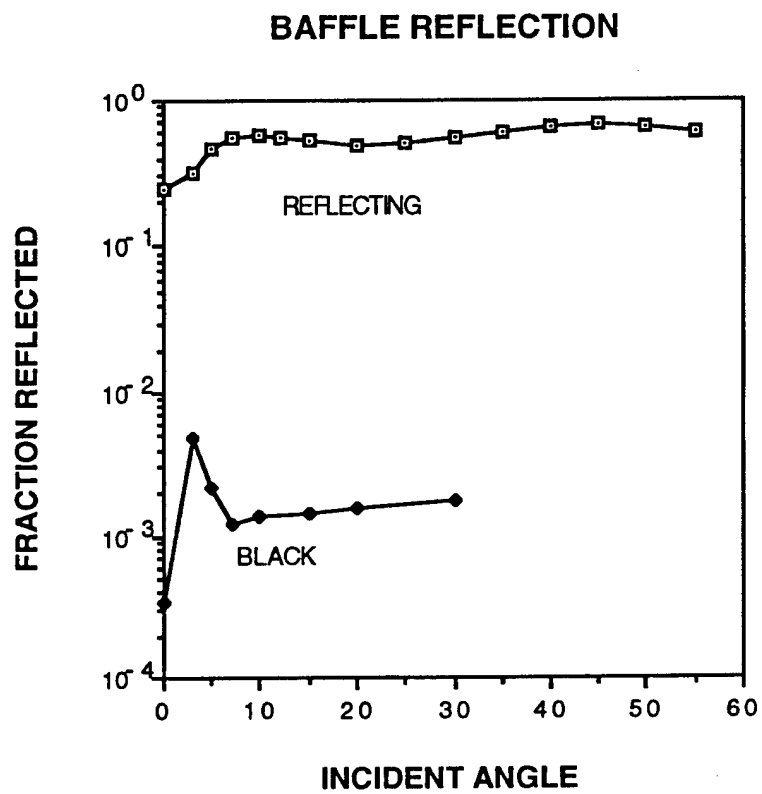


Figure 10. Fraction of energy reflected back out the entrance aperture as a function of incident angle for reflecting baffle and black baffle.

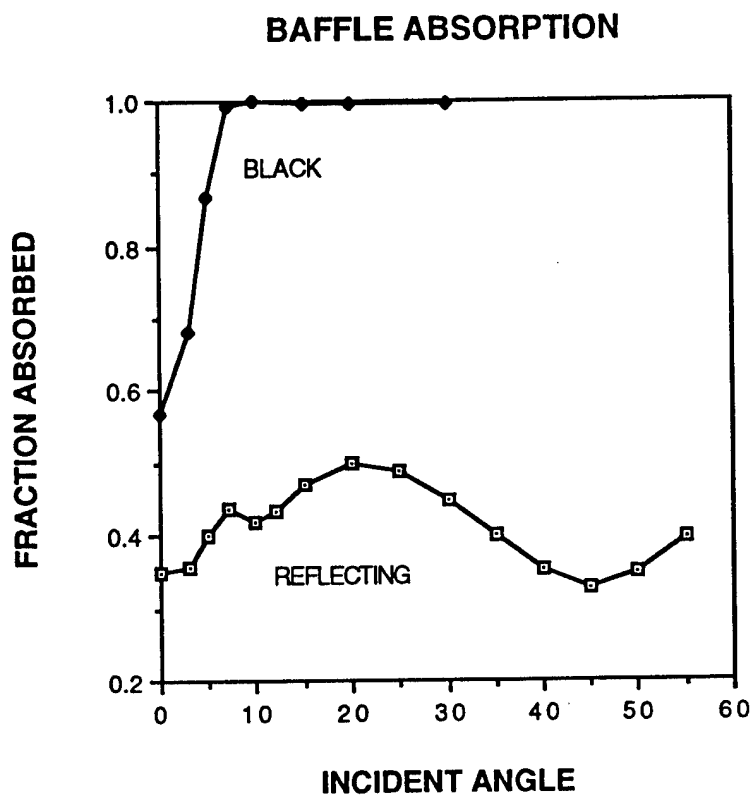


Figure 11. Fraction of energy absorbed as function of incident angle for reflecting baffle and black baffle.

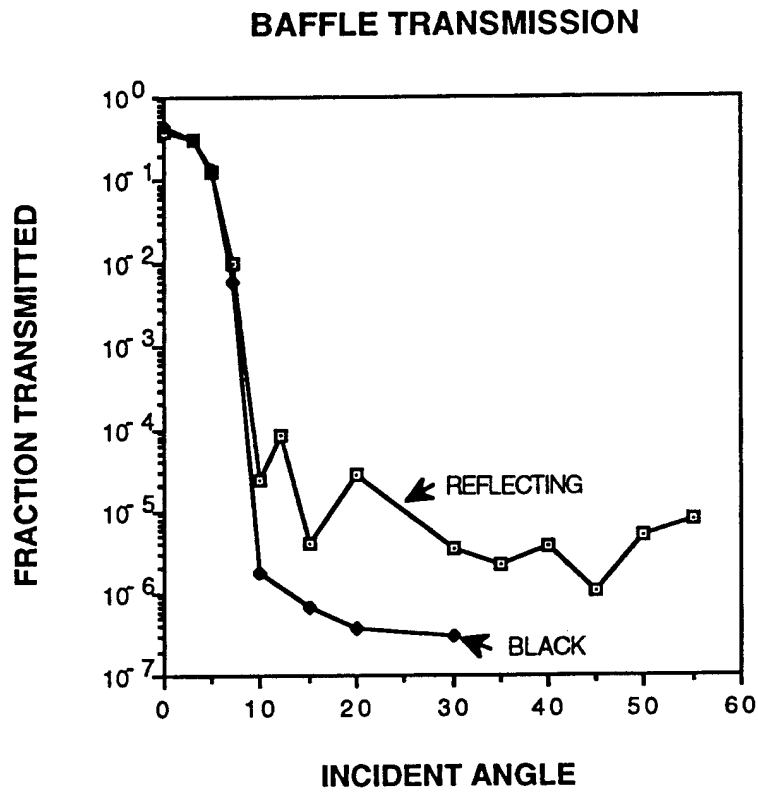


Figure 12. Fraction of energy transmitted as a function of incident angle for reflecting baffle and black baffle.

of the entrance aperture were coated with black diffuse paint with a 5 percent diffuse reflection and 95 percent absorption. All surfaces in the baseline black baffle had 95 percent absorption and 5 percent diffuse reflection.

Figure 10 shows the fraction of energy entering the entrance aperture of the baffle that was reflected back out the entrance aperture. Beyond the baffle cutoff angle of about 7 degrees, the retroreflecting baffle reflects about 60 percent of the energy while the black baffle reflects only about 0.1 percent. Most of the energy that is not reflected by the baffle is absorbed by the black surfaces in the baffle, and a small amount passes through the exit aperture. Figure 11 shows that the reflecting baffle absorbs about 40 percent while almost all the energy is absorbed by the black baffle. The fraction of energy transmitted through the baffle to the exit aperture is given in Figure 12. At angles greater than the baffle cutoff angle, the reflecting baffle transmits about a factor of 10 more energy than the black baffle. This is a somewhat discouraging result since it was hoped that the reflecting baffle would actually transmit less energy than the black baffle. The reason the reflecting baffle has higher transmission was not determined but could be caused by the two-reflection rays from the cube corners that tend to be directed into the baffle toward the exit.

The reflecting baffle is able to reflect a substantial fraction of the entering off-axis energy. This would result in reduced refrigeration requirements, but unfortunately the reflecting baffle transmits more off-axis energy to the exit aperture. Baffle transmission of off-axis rays has the ultimate effect of leaking off-axis radiation into the field of view. In an infrared sensor, the baffle is followed by an infrared telescope that typically has one or more field stops that define the field of view of the sensor. The off-axis rays that are transmitted through the baffle enter the telescope outside the field of view and the majority will image outside the field stop opening and be prevented from reaching the

sensor detector. However, the telescope mirror surfaces will scatter a small fraction of the off axis rays into the field of view, and these rays will pass through the field stop and ultimately reach the detector. For atmospheric earth limb measurements the off-axis source is the earth and lower atmosphere and the off-axis leakage is known as non-rejected earth radiance (NRER). The radiance from the upper atmosphere falls off rapidly with increasing tangent altitude for most emitting species, but the non-rejected earth radiance falls off much more slowly. At low tangent altitudes the atmospheric emission within the field of view of the sensor will dominate. As the altitude increases, the non-rejected earth radiance becomes a larger fraction of the total signal and eventually dominates the signal.

The next baffle that was evaluated was identical to the first but with cube corner arrays having some diffuse reflection and absorption. Figures 13, 14 and 15 show the results for a reflecting baffle having cube corner material with 28 percent total diffuse reflection for three-reflection rays and 3 percent absorption at each reflection. This represents cube corner material similar the 3M sample evaluated but with considerably less absorption. Absorption of 3 percent was assumed, rather than the measured 16 percent, since it was assumed that a reflective coating with 3 percent absorption should be obtainable.

The fraction of energy reflected has decreased to about 40 percent as compared to 60 percent for the baffle with ideal cube corner arrays. This is an encouraging result since even with the assumed high level of diffuse scatter the baffle is still able to reflect a substantial fraction of the incident radiation. It is certainly feasible that higher quality cube corner arrays could be manufactured that would have lower scatter levels than the array we measured. The fraction of energy absorbed by the baffle has increased to about 60 percent as compared to 40 percent for the baffle with ideal cube corner arrays. The fraction of energy

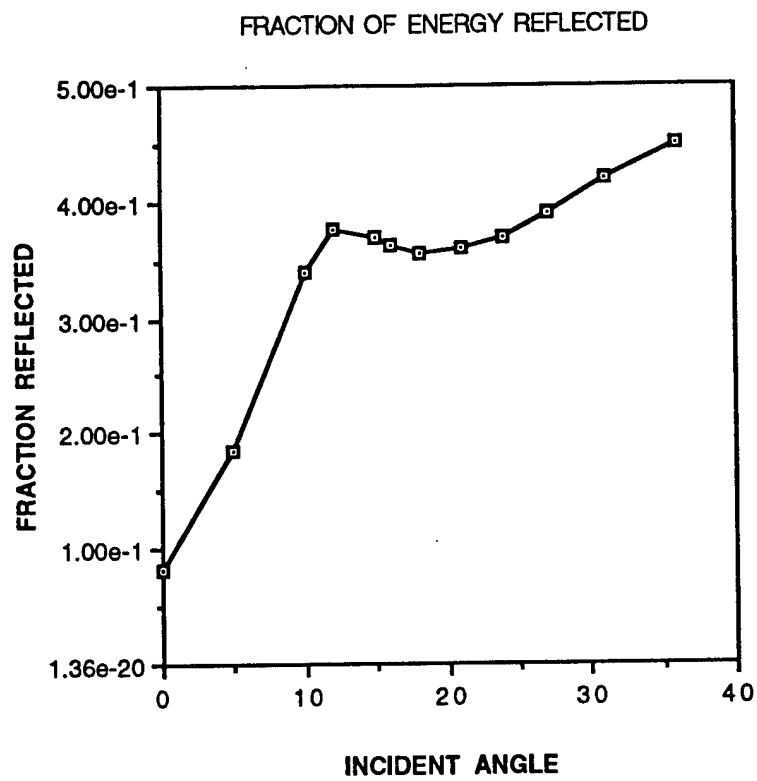


Figure 13. Fraction of energy reflected back out entrance aperture as a function of incident angle.

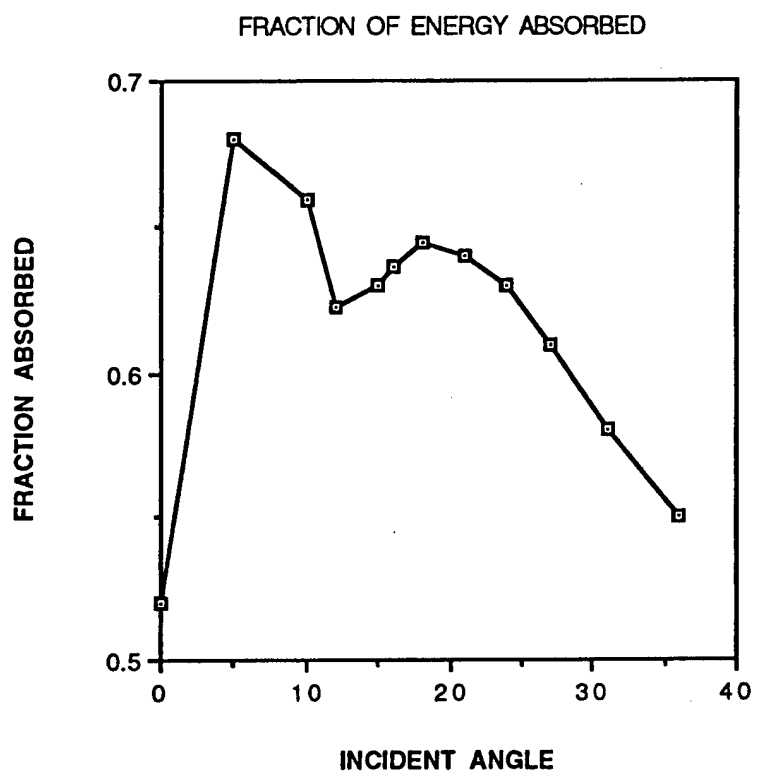


Figure 14. Fraction of energy absorbed by baffle as a function of incident angle.

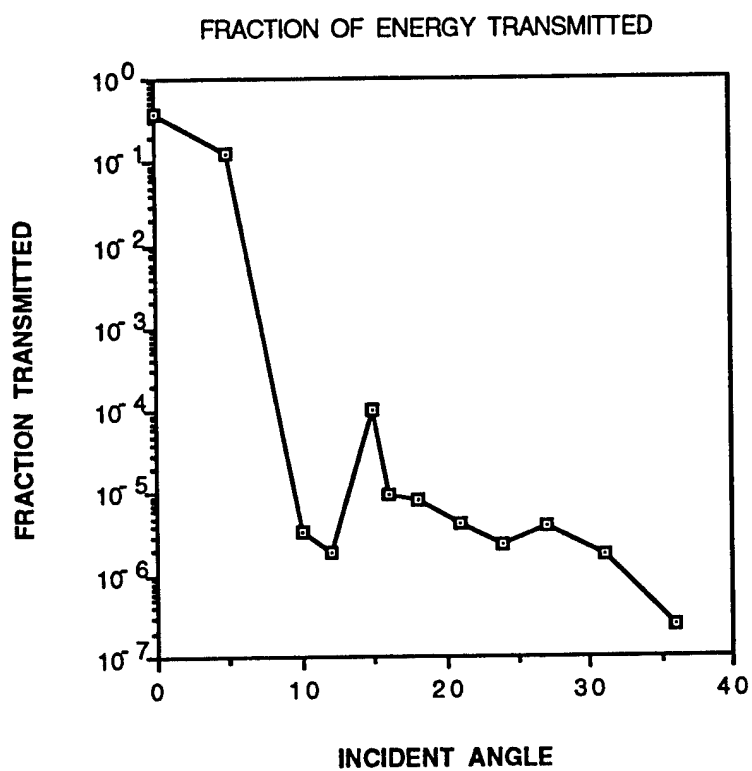


Figure 15. Fraction of energy transmitted through baffle as a function of incident angle.

transmitted to the exit aperture is similar to the levels calculated for the ideal reflective baffle and remains a factor of 10 higher than the black baffle.

The back side of the entrance aperture in the retroreflective baffles evaluated above accounts for a significant fraction of the total absorbed energy especially at large off-axis angles. Variations in the entrance aperture were investigated that would reduce the absorbed energy. One design that results in significantly reduced absorbed off-axis energy is shown in Figure 16. The length-to-exit diameter ratio has been reduced to about 4. The flat entrance aperture has been replaced with an aperture that is tilted toward the entrance and is reflective rather than black. The first retroreflective baffle is tilted more into the baffle so that two-reflection rays from the first baffle are reflected back out the entrance. The front surface of each baffle is covered with reflective cube corners as before, and the back side is coated with black diffuse paint. The PC-GUERAP calculations of fraction of energy absorbed as a function of entrance angle are shown in Figure 17. The reflected energy fraction peaks at 0.86 at an angle of 55 degrees. The fraction of energy transmitted through the baffle is shown in Figure 18 and is still significantly higher than the fraction transmitted by a black baffle having the same length to diameter ratio.

4. SUMMARY AND CONCLUSIONS

The use of small cell cube corner reflector arrays on the front surface of baffle rings can reduce the energy absorbed by the baffle by about a factor of 2 to 5 for the baffle designs we considered. This results in significantly reduced cooling requirements. A sensor cooled by a liquid or solid cryogen would use less cryogen for each minute of measurement time. The sensor could either be made

smaller or the measurement time extended. A sensor cooled with a refrigeration system would require a smaller refrigeration unit with a resulting savings in weight and power.

The off-axis leakage of the reflective baffles we modeled is about a factor of 10 higher than the off-axis leakage of a black absorbing baffle having the same length-to-diameter ratio. This is undesirable for certain applications such as measurement of spectral emission from the atmosphere at high tangent altitudes (above 100 km). The increased off-axis leakage would increase the non-rejected earth radiance which could result in spectra that are contaminated by emission and absorption features due to the earth and lower atmosphere.

The increased off-axis leakage is probably not much of a problem for a surveillance sensor looking for point source targets. Such a sensor typically filters out low spatial frequency background structure. The off-axis leakage would most likely only contain very low frequency spatial structure that would be eliminated by the filter.

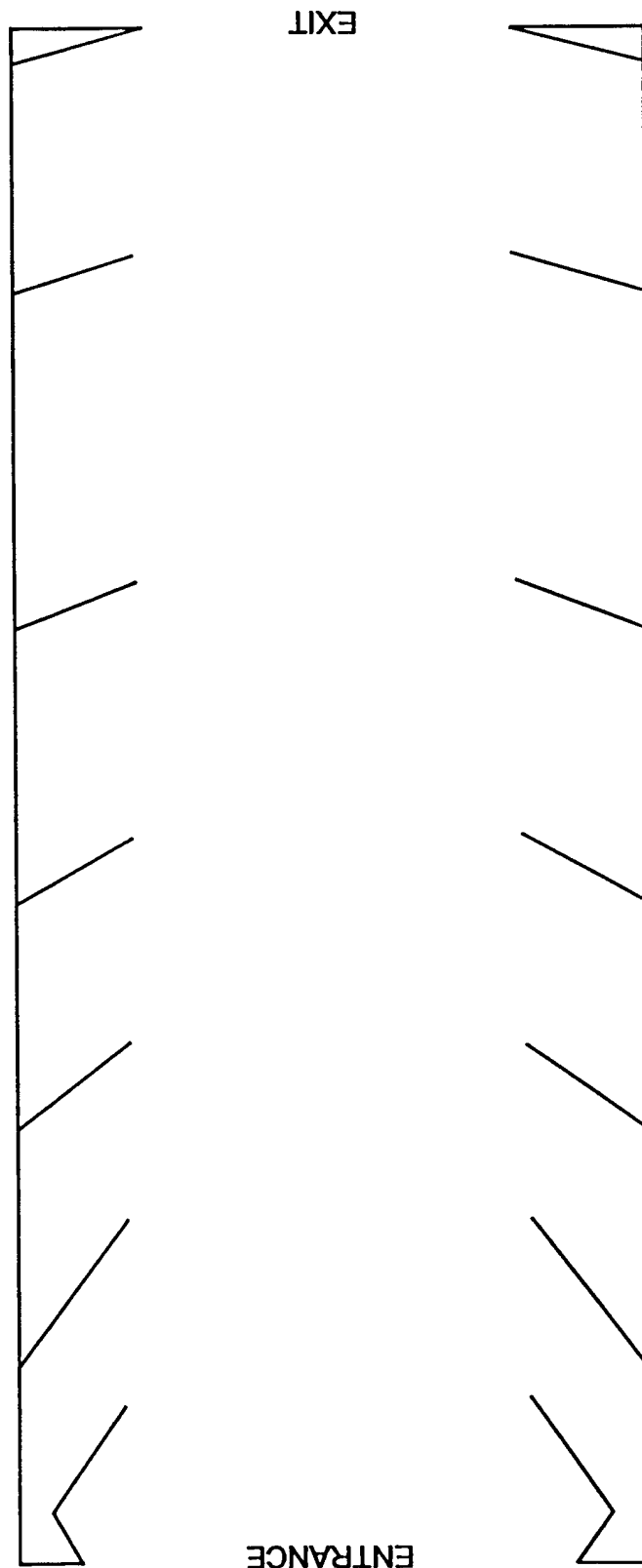


Figure 16. Modified baffle design having a reflecting entrance aperture that reflects two-reflection rays from the first retroreflecting baffle back out the entrance.

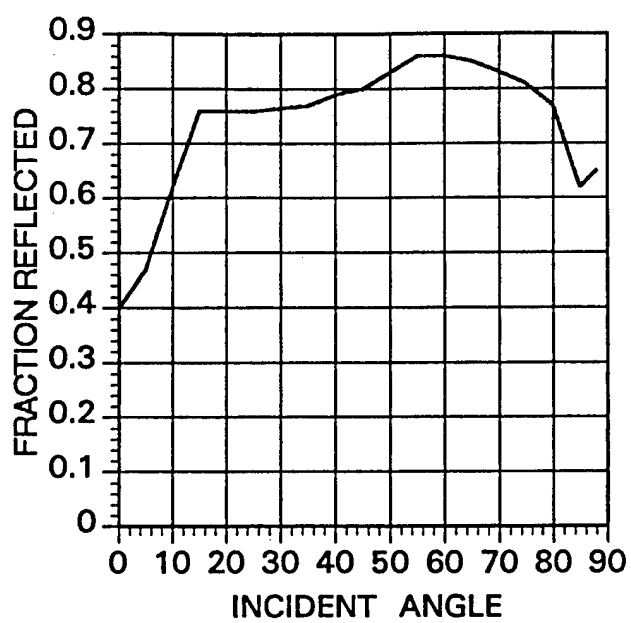


Figure 17. Fraction of energy reflected back out the entrance for the baffle shown in Figure 16.

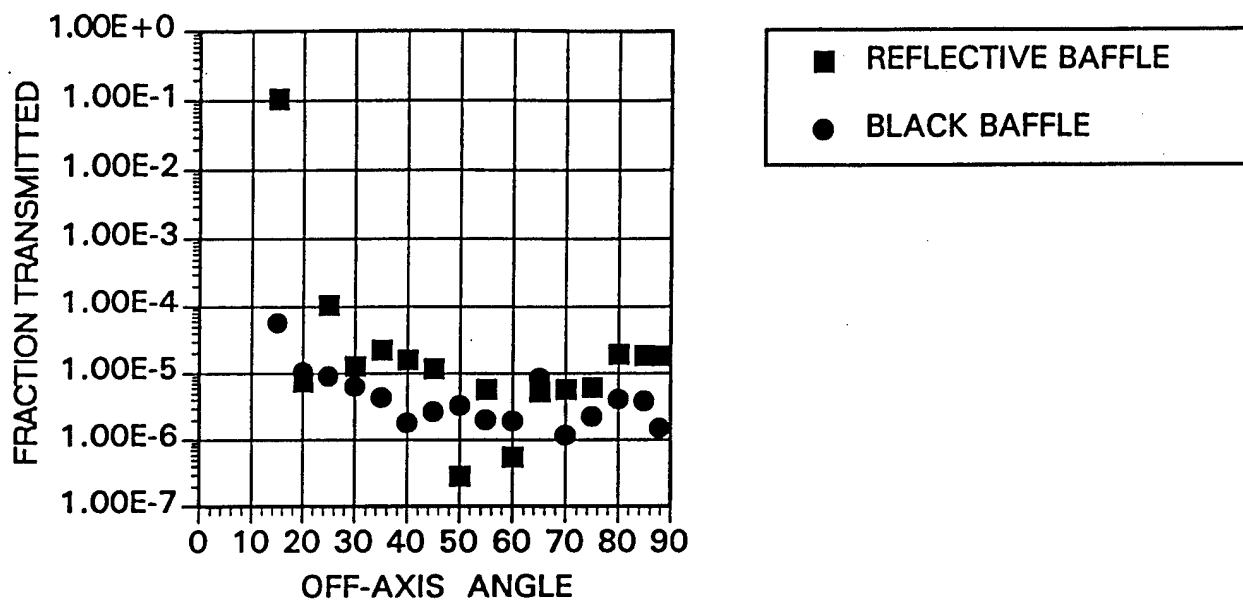


Figure 18. Fraction of energy transmitted to the exit aperture for the baffle shown in Figure 16 compared with the fraction transmitted by a standard black baffle.

References

1. Sears, F. R., (1949), *Optics*, Addison-Wesley Publishing Company, Inc., Reading Massachusetts, 37.
2. Chipman, R. A., Shamir, J., Caufield, H. J., and Zhou, Q., (1988), Wavefront Correcting Properties of Corner-Cube Arrays, *Applied Optics*, **27**, No. 15:3203
3. Wolf, W. L., and Zissis, G. J., eds., (1985), *The Infrared Handbook*, Office of Naval Research, Washington, DC, 23-7.
4. Barrett, H. H., and Jacobs, S. F., (1979), Retroreflective Arrays as Approximate Phase Conjugators, *Opt. Lett.*, **4**:190.
5. Jacobs, S. F., (1982), Experiments With Retrodirective Arrays, *Optical Engineering*, **21**, No. 2:281.